applied sciences

MDPI

Article

Stereo-DIC Measurements of a Vibrating Bladed Disk: In-Depth Analysis of Full-Field Deformed Shapes

Paolo Neri *, Alessandro Paoli and Ciro Santus

Department of Civil and Industrial Engineering, University of Pisa, Largo Lucio Lazzarino, 2, 56122 Pisa, Italy; alessandro.paoli@unipi.it (A.P.); ciro.santus@unipi.it (C.S.)
* Correspondence: paolo.neri@dici.unipi.it

Abstract: Vibration measurements of turbomachinery components are of utmost importance to characterize the dynamic behavior of rotating machines, thus preventing undesired operating conditions. Local techniques such as strain gauges or laser Doppler vibrometers are usually adopted to collect vibration data. However, these approaches provide single-point and generally 1D measurements. The present work proposes an optical technique, which uses two low-speed cameras, a multimedia projector, and three-dimensional digital image correlation (3D-DIC) to provide full-field measurements of a bladed disk undergoing harmonic response analysis (i.e., pure sinusoidal excitation) in the kHz range. The proposed approach exploits a downsampling strategy to overcome the limitations introduced by low-speed cameras. The developed experimental setup was used to measure the response of a bladed disk subjected to an excitation frequency above 6 kHz, providing a deep insight in the deformed shapes, in terms of amplitude and phase distributions, which could not be feasible with single-point sensors. Results demonstrated the system's effectiveness in measuring amplitudes of few microns, also evidencing blade mistuning effects. A deeper insight into the deformed shape analysis was provided by considering the phase maps on the entire blisk geometry, and phase variation lines were observed on the blades for high excitation frequency.

Keywords: bladed disk vibration; digital image correlation; low-speed cameras; downsampling; mistuning

Citation: Neri, P.; Paoli, A.; Santus, C. Stereo-DIC Measurements of a Vibrating Bladed Disk: In-Depth Analysis of Full-Field Deformed Shapes. *Appl. Sci.* **2021**, *11*, 5430. https://doi.org/10.3390/app11125430

Academic Editor: César M. A. Vasques

Received: 12 May 2021
Accepted: 7 June 2021
Published: 11 June 2021

1. Introduction

The experimental characterization of bladed disks (or blisks) dynamics is a critical task in turbomachinery for avoiding potential resonances and harsh startup and shutdown [1]. Bladed disks are usually characterized by many vibration modes which need to be recognized and investigated both with Finite Element (FE) analysis and through a dedicated experimental analysis [2]. These modes can be critically excited by different engine orders which induce resonances [3].

Any bladed disk has a nominal shape which is in principle perfectly cyclic. However, small deviations of this symmetry property are unavoidable, due to small manufacturing imperfections or even material inhomogeneities [4]. This deviation from the nominal shape is usually referred to as "mistuning" and can be distinguished into just random mistuning and intentional mistuning, and this latter is introduced to mitigate the vibrations of the random mistuning itself [4,5]. A dedicated modeling is therefore required, usually based on reduced-order models [5–7], and this can provide a tool for the optimization of the intentional mistuning pattern [8,9]. The mistuning can even be obtained by applying a coating on the blades with an intentional different thickness on each blade, which can be easily controlled at the manufacturing stage [6]. Even two coating layers can be applied on each blade for a more effective intentional mistuning [10]. The main role of these coatings is to introduce a damping effect, indeed damping hard coating materials are employed, and damping mistuning is obtained, which can be modeled and ultimately optimized.

However, the coating affects also the mass and the stiffness of the blades, which can be more accurately considered, as pointed out by Yan et al. [11].

FE investigation on blisks efficiently models the nominal vibration modes and their frequencies, regardless of any mistuning, and the FE modal analysis is run to provide the Singh's Advanced Frequency Evaluation (SAFE) diagram. This tool allows one to find the shape matching between the load harmonics and the modes and finally try to avoid the resonance matches [12]. This diagram was recently extended to the actual dynamic behavior of the blisks, by considering any possible mistuning, as proposed by Neri et al. [13]. However, a tailored experimental investigation is required to find the angular harmonic content of the bladed disks [14,15]. The proposed experimental technique requires a Laser Doppler Vibrometer (LDV), which measures the vibrating surface velocity along the specific direction of the laser beam and at the laser spot, thus providing just a point measurement though quite accurate. The use of accelerometers or strain gauges, providing either the acceleration or the local deformation of the structure, respectively, are valid alternative techniques. However, they are still measuring a single point of the structure.

Multiple measurement points can be alternatively recorded with a traveling LDV, as proposed by Bertini et al. [14], such as by using a robotic station for the accurate positioning of the laser beam with respect to the complex bladed disk geometry. Other techniques are obviously available for posing the LDV in a defined position with respect to the component, for example, by combining a camera and the CAD model, as proposed by Sels et al. [16]. However, after considering the number of blisk blades, if several measurement points are dedicated to each sector, the total number of positioning steps is too large, thus the whole procedure is quite time consuming. Scanning LDV (SLDV), or Continuously Scanning LDV (CSLDV), could provide another similar approach, by performing a scan along a linear path [17] or a circular path by means of two mirrors aligned according to a specific arrangement [18,19]. However, SLDV signal is much stronger when the beam direction is approximately aligned with the surface normal, which is not feasible in complex 3D blisks geometry. Additionally, since SLDV are 1D sensors, three separate devices would be needed to obtain 3D information, requiring a proper calibration and control strategy to ensure that all the sensors point at the same location over time. This results in complex and expensive hardware setups.

For these reasons, a *vision-based* system can be a valid alternative solution to capture the modal shapes of industrial bladed disks, performing a *full-field* dynamic acquisition of the displacements. The Digital Image Correlation (DIC), augmented by the stereoscopic feature, stereo-DIC or 3D-DIC [20], is quite effective for this application mainly for two reasons: the high complexity of the target geometry, as mentioned before, and the large or almost complete accessibility of the blade surfaces, at least for the unshrouded blisks, such as that tested in this work. To obtain a three-dimensional displacement map, stereo image pairs of the vibrating target are simultaneously acquired with two synchronized cameras [21,22]. An interesting comparison between stereo-DIC and 3D scanner LDV was provided by Reu et al. [23]. The three-dimensional LDV is obtained with three scanning laser heads to obtain the velocity vector, instead of just a component. The obtained results were quite accurate both in terms of frequencies and modal shapes, although only a simple plate was considered as test article. However, significant differences can be observed in terms of acquisition and analysis times as well as costs.

Acquisitions with high frames per second (fps) are usually required in 3D-DIC to identify rigid and small structures, resulting in high-frequency modes and fast harmonic responses. Therefore, two high-speed cameras are required for stereo vision, and they need to be synchronized in time, even within nanoseconds [22]. Beberniss and Ehrhardt [24] used two cameras with a maximum frame rate of 5000 fps, which obviously implies a Nyquist frequency of 2500 Hz, and a harmonic at 1230 Hz was indeed properly detected. Yu and Pan [25] just used a single high-speed camera and a setup involving four planar mirrors to compensate the single point of vision and still obtain a three-dimensional reconstruction

of the vibration response. Their camera was set at 500 fps, having a target maximum natural frequency of just 55 Hz. Durand-Texte et al. [26] again used a four-mirror setup for achieving a pseudo-stereo system, using a very high-speed camera up to 12,500 fps. They measured frequency response functions (FRF) up to 1000 Hz, and the modal shape reconstruction was quite successful for a mode at frequency 600 Hz, thus much lower than the Nyquist frequency.

On the contrary, the subsampling strategy, or alternatively mentioned as downsampling, can be performed to overcome the Nyquist rate limitation [27–29]. If the signal to be reconstructed is just a sinusoidal harmonic, a sampling time can be chosen as slightly different (usually higher) than an integer multiple of the period. In principle, according to this approach, any vibration frequency could be measured, but two issues should be considered. The harmonic content of the signal must be purely sinusoidal, and this can be obtained as the result of a single harmonic response, provided that the exciting load is again a pure sine function and any nonlinearity is avoided, especially in terms of boundary constraints. The other requirement is that the exposure time of the camera, at maximum shutter speed, is short enough with respect to the vibration period.

In this paper, the 3D-DIC was applied to a bladed disk and the downsampling strategy was adopted to find the deformed shape of this structure, up to the high-frequency range in the order of several kHz. Two low frame-rate cameras, with a fast shutter time, have been assembled in a stereo set-up, and a digital projector has been used to project a structured light pattern, thus strengthening the stereo matching and enhancing the 3D-DIC reconstruction. Additionally, a time-domain filtering has been implemented to enhance relevant harmonic contributions. The description of the deformed shapes at different resonance frequencies was provided. Some considerations on the response of the vibrating blisk are finally drawn and discussed by observing both amplitude and phase distributions.

2. Optical System Setup

The measurement system presented here was devised to obtain high-speed full-field 3D measurement by exploiting a stereo optical setup. To this extent, two CMOSIS cameras were used, equipped with a 2024 × 2024, 1-inch black and white sensor (Optomotive TREX). The maximum available frame rate of the cameras was 178 fps. This would limit the application of the sensors to 89 Hz, according to the Nyquist–Shannon theorem if transient signals would be acquired. However, it was proven that a low speed sensor can be used to acquire high-frequency signals, provided that a single harmonic component is excited, as recently performed by Barone et al. [27–29]. In this scenario, the frame rate does not represent a limitation anymore. Whereas, in order to avoid blur images, the shutter time is critical. This can be solved either by using a short shutter time or by introducing a fast illumination source which provides short time light pulses. Since this latter solution required additional costly hardware, the first approach was adopted in this work, by exploiting the minimum shutter time of the cameras, which was 2 µs. This really short Δt was fifty times lower then the period of a 10 kHz signal, which was assumed as the highest frequency of interest for the system. Furthermore, this ratio was similar to other examples in the literature, such as Endo et al. [30].

The two cameras were mounted on spherical joints, which were then fixed to a bar through a slide. This allowed for the fine tuning of the stereo system baseline and orientation. The cameras were also equipped with multifocal 1-inch, C-mount lenses (Azure Photonics 1632ZL5M, 5 Mpixel), which could be used to set aperture, zoom and focal length to adapt the system to different scales. Since a really short shutter time was used, high intensity light sources were needed. The StratusLed 100 W module (Version 3) was selected for this purpose, and four devices were equipped with parabolic reflectors and mounted on the same bar of the stereo system. The described setup is shown in Figure 1. The stereo system was calibrated exploiting a planar checkerboard and using the procedure described by Barone et al. [31].

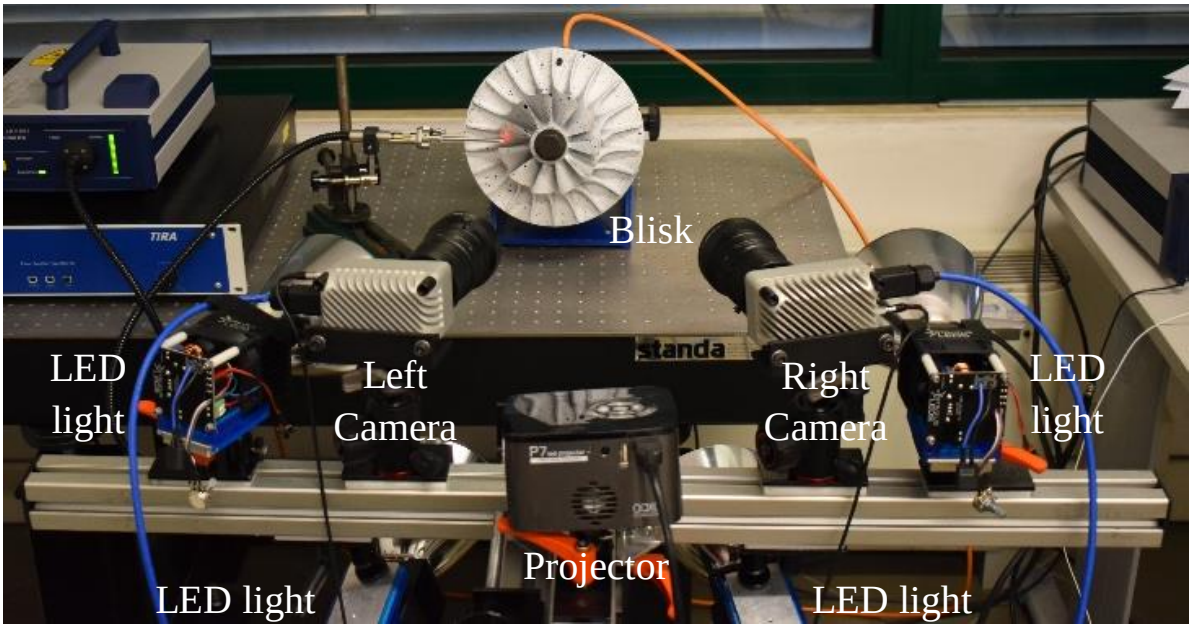

Figure 1. Optical setup of the stereo-DIC measurement system.

3. Digital Image Correlation Strategy

Since low frame-rate cameras are adopted, the downsampling approach was implemented, and the displacement signal was required to be composed by only one harmonic. In this scenario, it was possible to set the camera sampling frequency f_s to describe the chosen number of displacement periods (namely, n_p). This frequency was obtained with the following relation:

$$f_s = f_v(n_s/n_p)/(1 + (n_s/n_p)k) \quad (1)$$

where f_v is the actual signal frequency, n_s is the number of frames to be acquired, and k is any integer number. In this work, $n_p = 1$ was considered. The value of the integer k can be set arbitrarily high, knowing that higher values of k correspond to lower values of f_s. According to Equation (1), the downsampled acquired signal shows only one complete period of the vibration, thus allowing for the proper description of its amplitude. In order to achieve 3D measurements, the information from the two cameras was combined trough the stereo-triangulation method. To find the correspondence between left and right pixels (i.e., solving the stereo matching problem) a structured light approach was adopted exploiting the multimedia projector, to obtain an automate, robust and accurate solution. Once the correspondence between left and right pixels is known, as well as the stereo camera calibration parameters, it is possible to obtain 3D displacement maps starting from the 2D displacements measured by each camera. To speed up the process, the stereo matching problem was solved only once with the first couple of frames. The displacements were then tracked through Digital Image Correlation along the frame series on left and right cameras, without the need to repeat the stereo matching task. Additionally, a time domain filtering was applied to the raw camera frames to enhance the information related to the first harmonic of the time series (since $n_p = 1$ was used). This approach proved to be effective in previous research, saving elaboration time without losing reconstruction accuracy and obtaining smooth displacement maps. A full description of the image processing was recently presented by the authors in [32], along with the method validation. Both data acquisition and elaboration were performed with MATLAB software. The open source 2D DIC script was downloaded from the Mathworks website [33] and used to compute the left and right camera displacements. Custom scripts were developed for the further tasks: solve the stereo matching problem through fringe projection, then implement the time domain filtering, and eventually triangulate the 2D displacements to obtain the 3D maps.

4. Results

In order to assess the advantages of the proposed method, with respect to the conventional single-point systems, the harmonic response testing was performed on a blisk having eleven sectors, with a main blade and a splitter blade in each sector, and a maximum diameter of 220 mm. The blisk was painted in white, and a black speckle pattern was sprayed on the blade surface. A picture of the blisk, as acquired by the left camera during the acquisition, is shown in Figure 2a, and a number was assigned to each blade for easier referencing. As evident from the figure and due to the short shutter time, no blur is present in the image despite the high-frequency vibration of the blades (6357 Hz in this example). The figure also shows two reference frames: the Cartesian coordinate system of the camera and the cylindrical coordinate system of the blisk, which was introduced for a better understanding of the results, as shown below. To define this latter reference frame, three points of the point cloud were selected on the maximum diameter of the disk, placed at approximately 120° as shown in Figure 2b with red dots: the circle through these points was then computed, in order to obtain the center of the reference frame, which is placed on the axis of the blisk. Additionally, the normal to the plane defined by the three reference points was computed, which is aligned with the blisk axis (red arrow in Figure 2b). The counterclockwise direction was chosen for the rotational direction of the cylindrical reference system. Finally, the radial direction (i.e., the 0° location) was conventionally defined by the vector difference between the first two reference points.

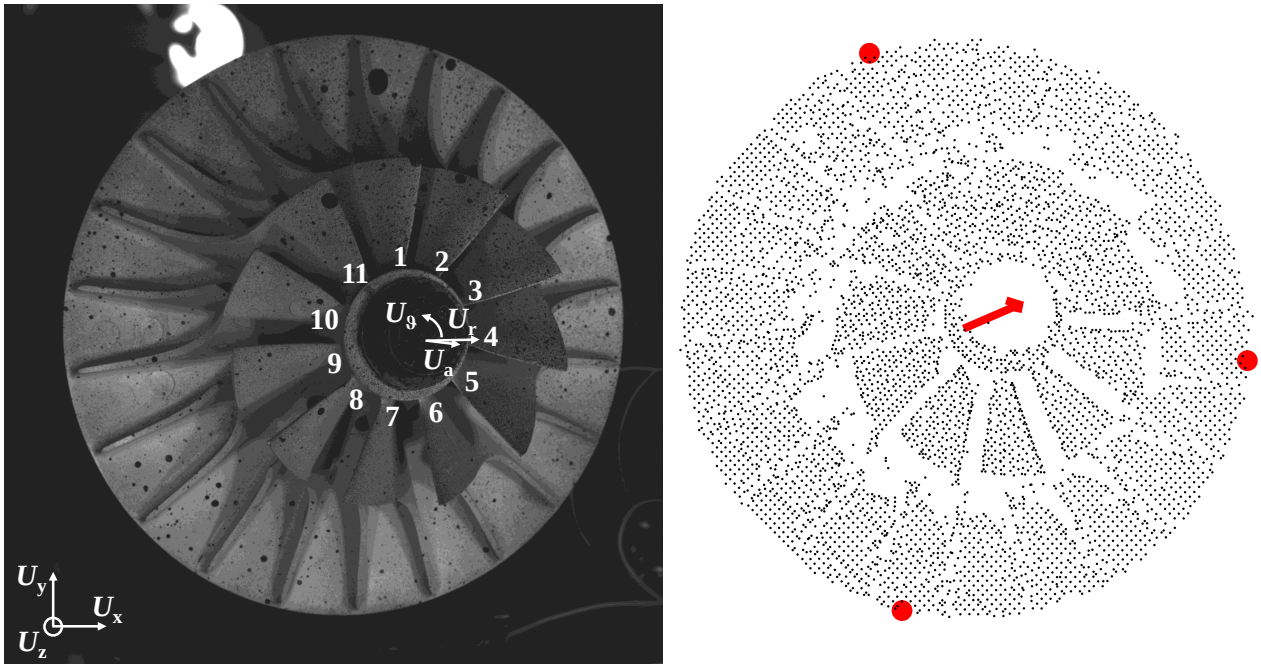

(a) (b)

Figure 2. (**a**) Acquisition of the tested blisk, by the left camera, during a high-frequency sine excitation. (**b**) Reference to three points on the disk outer diameter for the determination of the base plane and the axial direction as orthogonal to this plane.

The hub of the blisk was directly mounted on the plate of an electrodynamic shaker, and with this device it was possible to precisely set a sinusoidal excitation to the blisk. Different frequencies were tested to prove the effectiveness of the setup in the kHz range. As discussed in the literature, the kHz range represents a challenge even for those setups exploiting high-speed cameras. A preliminary analysis was performed by applying a sine sweep to the blisk, in the range 1–7 kHz, measuring the response of Blade 1 with an LDV sensor. This allowed researchers to find the main response peaks of the blisk, and thus to select some resonance frequencies, as shown in Figure 3.

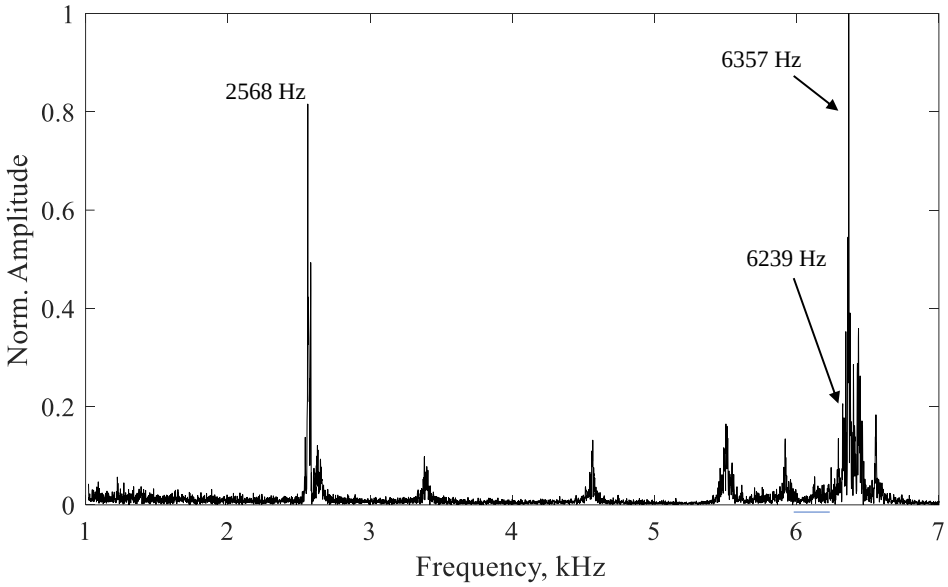

Figure 3. DFT of the single point LDV measurement obtained by blisk's random excitation.

A relatively low peak frequency of 2568 Hz was initially tested, which is however already much higher than the maximum frame rate available with the cameras of the present setup. Figure 4 shows the measured displacement maps, considering the components along the three directions of the blisk: radial, tangential and axial (U_r, U_ϑ and U_a, respectively).

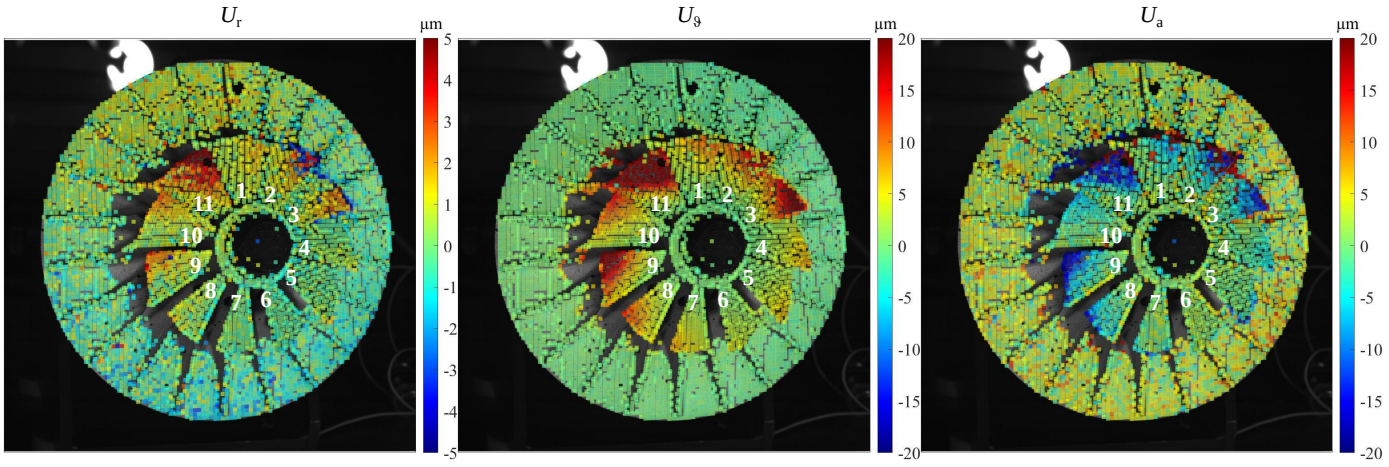

Figure 4. Displacement maps for the 2568 Hz excitation frequency, along the directions of the cylindrical reference system of the blisk.

These maps demonstrate that the 3D full-field measurements are properly achieved, despite the high vibration frequency and the low displacement amplitude, in the range of tens of microns. The full-field measurement allows for the reconstruction of the complete deformed shape of the blisk just with a single acquisition configuration, without requiring the movement of a single-point sensor in different locations. The images highlight that the higher response amplitude is measured at Blades 2, 3, 9 and 11, while the other blades experience much smaller displacements, thus denoting a certain mistuning level. Since a relatively low frequency is considered, the blade deformed shape has a low complexity level. This is evident because all the points of the blade move in phase to each other and with low gradients.

The test was then repeated at higher frequencies, to investigate the response of the modes to sinusoidal excitation of the hub in the range 6200–6400 Hz. The results for the testing frequency at 6239 Hz are reported in Figure 5, again in the cylindrical reference frame coordinates, showing a really smooth map for all the three directions.

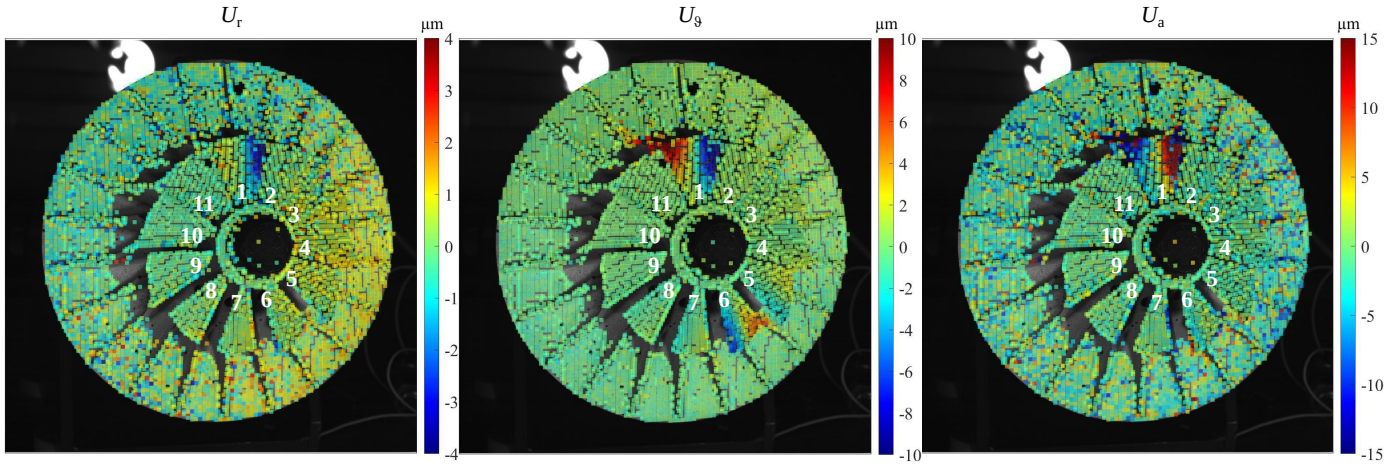

Figure 5. Displacement maps for the 6239 Hz excitation frequency, along the directions of the cylindrical reference system of the blisk.

The colorbars highlight that the axial direction is dominant in this harmonic response, showing that mainly Blade 1 is responding to the excitation. Nevertheless, radial and tangential displacement maps show that also Blade 6 is responding, at least in the in-plane direction, even if the displacement amplitude is much lower than the out-of-plane direction. This specific dynamic response emphasizes the need of 3D full-field measurements in this research field. Moreover, at this higher frequency a much more complex blade deformation is observed with respect to the previous at 2568 Hz mode. A nodal line can be noted on the blade surface, meaning that the points across this line of the same blade move out of phase. This behavior surely has an effect on the in operation stress levels and can also determine different resonance combination with the inlet fluid. A deeper insight in this deformed shape can be obtained, for example, by focusing the tangential displacement map to a range of ± 3 µm, as shown in Figure 6. This plot better emphasizes the presence of the nodal line in Blades 1 and 6. The same deformed shape feature can be additionally noted on Blades 5 and 7, even if with smaller amplitudes.

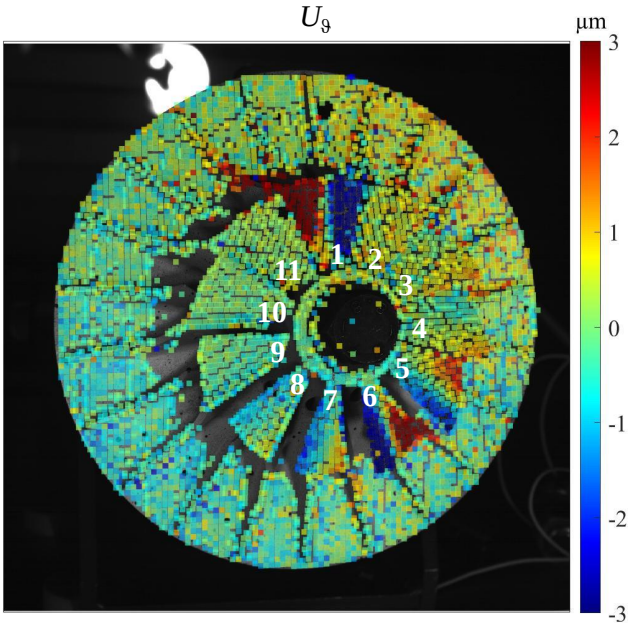

Figure 6. Displacement map for the excitation at the 6239 Hz with focused view of the tangential displacement.

Another high-frequency test investigated was 6357 Hz, and the results are reported in Figure 7. The displacement maps highlight that the blades presented quite similar deformed shape as the previous testing frequency at 6239 Hz, with one nodal line on the blade itself.

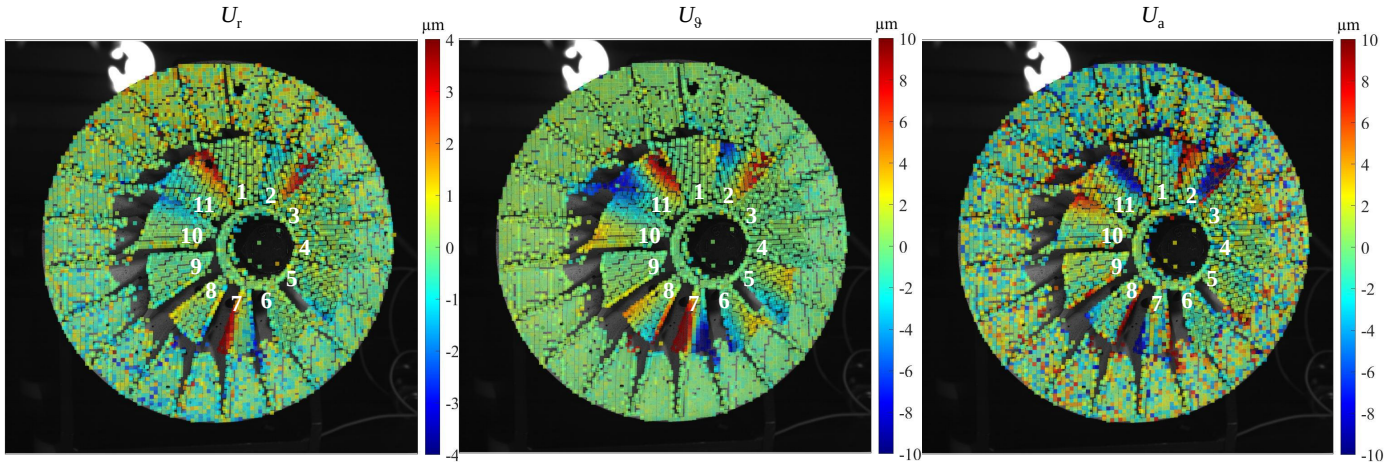

Figure 7. Displacement maps for the 6357 Hz excitation frequency, along the directions of the cylindrical reference system of the blisk.

Nevertheless, at this working frequency a different combination of blades is excited; since the main amplitude was found at Blade 11, the relevant responses were measured for Blades 2 and 7, while the other blades were approximately not responding. This is a peculiarity of the mistuned blisks, which presents several modes at different (but close) frequencies, featuring similar deformed shapes of the blades but different combinations of the responding blades.

In order to completely and precisely describe these harmonic responses, with single point techniques such as LDV, or even with CSLDV, a really long testing time would be needed, since several locations on each blade should be subsequently measured. Just a discrete description of the shape could be obtained otherwise, by observing a specific but limited set of positions.

5. Investigation of the Blade Deformed Shapes

The described testing procedure allows for the visualization of the harmonic response of the blisk under a sinusoidal excitation at any frequency. It is worth noting that, for lightly damped systems such as the blisks, the deformed shapes are expected to be characterized by all the points moving in phase or out of phase. This means that the phase difference between two points of the blisk should be approximately 0° or 180°. Nevertheless, in the case of blisks it is really common to have a certain mistuning level, which causes any theoretical tuned mode to split into two separate modes, having really close frequencies and asymmetric response amplitudes. These two modes, which are really close in frequency, cause the impossibility to separate their shapes during a harmonic response analysis. In this scenario, indeed, the measured deformed shape is the combination of the two mistuned modes. In addition to this, since at the investigated peak frequencies the two excited modes are close to the resonance, the excitation force and the responses are in general neither in phase nor out of phase, thus the phases are different for the two modes since their natural frequencies are slightly different. As a consequence, the measured deformed shape may present points with phase differences which are neither 0° nor 180°.

Both the amplitude asymmetry and the phase shifting can be investigated with the proposed setup. Since Equation (1) is used to set the cameras' frame rate ($n_p = 1$), the measured response describes one full period along the acquisition time. Thus, it is possible to compute the Discrete Fourier Transform (DFT) of each point of the displacement map and then evaluate the amplitude and the phase of the first harmonic for each measurement

point. This elaboration was performed, as an example, on the analyzed blisk for the tangential displacement of the tests at 2568 Hz and 6357 Hz frequencies, and the results are reported in Figure 8.

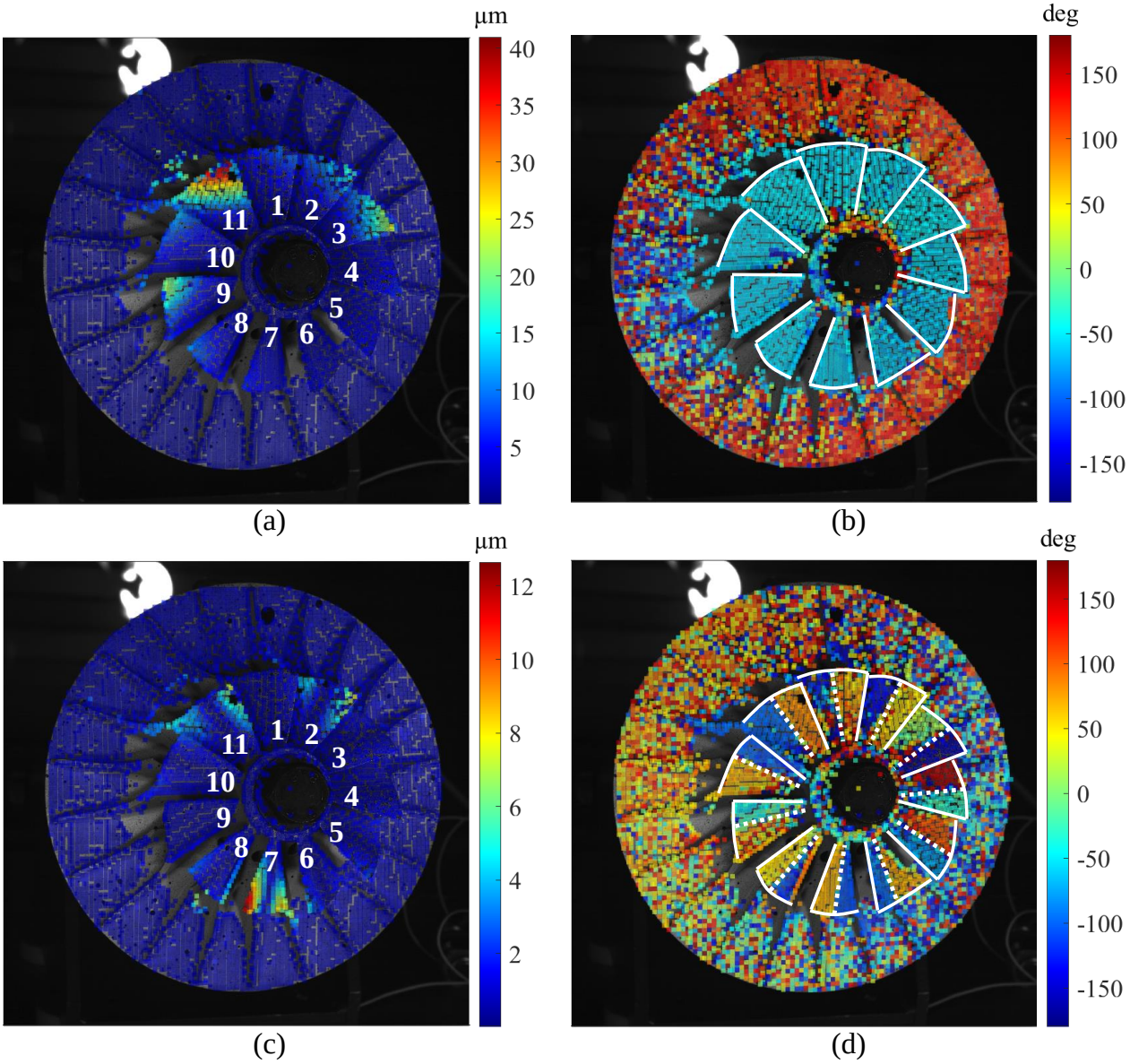

Figure 8. DFT elaborations of the test results: (**a**) amplitude at 2568 Hz, (**b**) phase at 2568 Hz, (**c**) amplitude at 6357 Hz, (**d**) phase at 6357 Hz.

In a theoretical scenario of perfectly symmetric and isolated modes, all the blades would show the same displacement amplitude for those modes with a Number of Nodal Diameters (NND) equal to zero, which are the modes experiencing the highest excitation when the load is applied at the hub of the blisk. On the contrary, mistuned blisks will show asymmetries in the amplitude maps and any phase value in the range 0–180°, as discussed before. To this extent, Figure 8a confirms that each blade has a different amplitude at 2568 Hz, thus denoting a certain mistuning level. On the other hand, Figure 8b shows that all the blades vibrate with the same phase of about −55°, while the disk is vibrating with a phase of about 125°, i.e., perfectly out of phase with respect to the blade. This distribution of the phases is common for the zero NND modes. Since all the points move in phase or out of phase, it is possible to state that only the shape of one mode was excited in this test. It is interesting to point out that the zero NND modes, in perfectly tuned blisks, are not

couples of degenerate modes. Thus, the presence of any mistuning can only determine amplitude asymmetry.

On the other hand, the test at 6357 Hz demonstrated a different behavior. Figure 8c again shows that the deformed shape was localized in few blades which had higher amplitudes, while Figure 8d shows that all the possible phase values between -180° and 180° were measured. In order to improve the readability, Figure 8b,d were enhanced by adding the white solid lines representing the blade contours. In Figure 8d dashed lines were additionally added, highlighting the presence of the nodal lines on the blades. Taking Blade 11 as an example, it is possible to note that the points on the left of the nodal line showed a phase of about -100°, while the points on the right resulted with a phase of about 80°, denoting that the two regions were vibrating out of phase. However, for example, the comparison between Blades 11 and 4 denotes that these two blades are neither in phase nor out of phase, since the phase difference is approximately 120°. Furthermore, a similar consideration can be drawn for the other blades. This observation demonstrates that the measured deformed shape is the combination of (at least) two different modes, which have the same shape in the blade domain but different combinations of responding blades along the circumference hoop.

As a final remark, from Figure 8 it is evident that the phase information was accurately reconstructed also for those blades with really small amplitudes. This demonstrates that the displacement information is somehow measured even at very small amplitudes.

6. Conclusions

The present work describes an experimental setup for obtaining full-field 3D displacement maps of high-frequency vibrating targets, through Digital Image Correlation. Two low frame-rate cameras were used to assemble a stereo system. This optical setup, in opposition to high-speed cameras, has much lower cost and higher resolution, which allows for higher sensitivity. On the other hand, the main limitation of the proposed approach is the need for downsampling, which imposes the constraint that the displacement signal under measurement necessarily consists of just a single sinusoidal harmonic. However, this can be easily obtained in many testing setups by using an electrodynamic shaker which can produce an accurate sinusoidal excitation load. Additionally, the camera shutter time must be short with respect to the measured signal period. A ratio of at least 50 between the signal period and the shutter time was used in this work. The described acquisition system was applied to the vibrational measurement of a blisk, and this allowed for the investigation of its mistuning level in the high-frequency range. To this extent, harmonic response analyses were performed at 2568 Hz, 6239 Hz and 6357 Hz to assess and compare the shape of these response peaks. It is worth noting that these frequency values in combination with the low response amplitudes, in the range of 10 μm, were not found in any previous research or in studies exploiting high-speed camera setups.

The obtained 3D displacement maps highlighted that all the observed harmonic responses could be explained as excited modes featuring relevant mistuning. This conclusion would be much more challenging to obtain with conventional single-point measurement techniques, since a great number of measurement points would be needed to fully describe the complex mode shapes. An insight in terms of the deformed shapes was additionally given by analyzing the amplitude and the phase maps. This investigation highlighted that in the case of blisks it is really difficult, or merely impossible, to separate different mode shapes with a harmonic response analysis. The reason for this is the mistuning effect which splits the degenerate modes in two separate, asymmetric and close in frequency modes.

In principle, the described measurement system could be used to estimate the blisk damping, by comparing the response and the load amplitude, provided that the excitation force is measured during the test. However, this phenomenon is generally quite low for this kind of structure, thus an accurate detection of the damping is expected to be a challenging task and can be considered for a future investigation.

Author Contributions: Conceptualization, P.N., A.P. and C.S.; software, P.N.; validation, P.N., A.P. and C.S.; writing—original draft preparation, P.N.; writing—review and editing, A.P. and C.S. All authors have read and agreed to the published version of the manuscript.

Funding: This research received no external funding.

Data Availability Statement: It is not applicable.

Conflicts of Interest: The authors declare no conflict of interest.

Abbreviations

The following abbreviations are used in this manuscript:

DIC	Digital Image Correlation.
3D-DIC	Three-dimensional or stereo-DIC.
LDV	Laser Doppler Vibrometer.
CSLDV	Continuously Scanning LDV.
SAFE	Singh's Advanced Frequency Evaluation (diagram).
DFT	Discrete Fourier Transform.
NND	Number of Nodal Diameters.

References

1. Wilcox, E. Vibration Analysis for Turbomachinery. In Proceedings of the 45th Turbomachinery Symposium, Houston, TX, USA, 12–15 September 2016. [CrossRef]
2. de Cazenove, J.; Cogan, S.; Mbaye, M. Finite-Element Modelling of an Experimental Mistuned Bladed Disk and Experimental Validation. In *Volume 7B: Structures and Dynamics*; American Society of Mechanical Engineers: San Antonio, TX, USA, 2013. [CrossRef]
3. Kammerer, A.; Abhari, R.S. Experimental Study on Impeller Blade Vibration during Resonance—Part I: Blade Vibration Due to Inlet Flow Distortion. *J. Eng. Gas Turbines Power* **2008**, *131*. [CrossRef]
4. Beirow, B.; Figaschewsky, F.; Kühhorn, A.; Bornhorn, A. Modal Analyses of an Axial Turbine Blisk With Intentional Mistuning. *J. Eng. Gas Turbines Power* **2017**, *140*. [CrossRef]
5. Martel, C.; Sánchez-Álvarez, J.J. Intentional mistuning effect in the forced response of rotors with aerodynamic damping. *J. Sound Vib.* **2018**, *433*, 212–229. [CrossRef]
6. Khemiri, O.; Martel, C.; Corral, R. Asymptotic description of damping mistuning effects on the forced response of turbomachinery bladed disks. *J. Sound Vib.* **2013**, *332*, 4998–5013. [CrossRef]
7. Wang, S.; Bi, C.X.; Zheng, C.J. A Reduced-Order Model for the Vibration Analysis of Mistuned Blade–Disc–Shaft Assembly. *Appl. Sci.* **2019**, *9*, 4762. [CrossRef]
8. Han, Y.; Murthy, R.; Mignolet, M.P.; Lentz, J. Optimization of Intentional Mistuning Patterns for the Mitigation of the Effects of Random Mistuning. *J. Eng. Gas Turbines Power* **2014**, *136*. [CrossRef]
9. Tan, Y.; Zang, C.; Petrov, E.P. Mistuning sensitivity and optimization for bladed disks using high-fidelity models. *Mech. Syst. Signal Process.* **2019**, *124*, 502–523. [CrossRef]
10. Gao, J.; Gao, Y.; Yan, X.; Jiang, J.; Xu, K.; Sun, W. Damping mistuning effect of the hard-coating-based intentional mistuning techniques on mistuned blisks and its mechanism. *Aerosp. Sci. Technol.* **2020**, *101*, 105848. [CrossRef]
11. Yan, X.; Gao, J.; Zhang, Y.; Xu, K.; Sun, W. Modeling method of coating thickness random mistuning and its effect on the forced response of coated blisks. *Aerosp. Sci. Technol.* **2019**, *92*, 478–488. [CrossRef]
12. Bertini, L.; Neri, P.; Santus, C.; Guglielmo, A.; Mariotti, G. Analytical investigation of the SAFE diagram for bladed wheels, numerical and experimental validation. *J. Sound Vib.* **2014**, *333*, 4771–4788. [CrossRef]
13. Neri, P.; Bertini, L.; Santus, C.; Guglielmo, A. Generalized SAFE Diagram for Mistuned Bladed Disks. *J. Eng. Gas Turbines Power* **2019**, *141*. [CrossRef]
14. Bertini, L.; Neri, P.; Santus, C.; Guglielmo, A. Automated Experimental Modal Analysis of Bladed Wheels with an Anthropomorphic Robotic Station. *Exp. Mech.* **2017**, *57*, 273–285. [CrossRef]
15. Bertini, L.; Neri, P.; Santus, C.; Guglielmo, A. One Exciter per Sector Test Bench for Bladed Wheels Harmonic Response Analysis. In *Volume 7B: Structures and Dynamics*; American Society of Mechanical Engineers: Charlotte, NC, USA, 2017; doi:10.1115/gt2017-63628. [CrossRef]
16. Sels, S.; Vanlanduit, S.; Bogaerts, B.; Penne, R. Three-dimensional full-field vibration measurements using a handheld single-point laser Doppler vibrometer. *Mech. Syst. Signal Process.* **2019**, *126*, 427–438. [CrossRef]
17. Stanbridge, A.B.; Martarelli, M.; Ewins, D.J. Measuring area vibration mode shapes with a continuous-scan LDV. *Measurement* **2004**, *35*, 181–189. [CrossRef]
18. Halkon, B.J.; Rothberg, S.J. Vibration measurements using continuous scanning laser vibrometry: Advanced aspects in rotor applications. *Mech. Syst. Signal Process.* **2006**, *20*, 1286–1299. [CrossRef]

19. Giuliani, P.; Maio, D.D.; Schwingshackl, C.W.; Martarelli, M.; Ewins, D.J. Six degrees of freedom measurement with continuous scanning laser doppler vibrometer. *Mech. Syst. Signal Process.* **2013**, *38*, 367–383. [CrossRef]
20. Schreier, H.; Orteu, J.J.; Sutton, M.A. *Image Correlation for Shape, Motion and Deformation Measurements*; Springer: New York, NY, USA, 2009. [CrossRef]
21. Helfrick, M.N.; Niezrecki, C.; Avitabile, P.; Schmidt, T. 3D digital image correlation methods for full-field vibration measurement. *Mech. Syst. Signal Process.* **2011**, *25*, 917–927. [CrossRef]
22. Sutton, M.A. Computer Vision-Based, Noncontacting Deformation Measurements in Mechanics: A Generational Transformation. *Appl. Mech. Rev.* **2013**, *65*. [CrossRef]
23. Reu, P.L.; Rohe, D.P.; Jacobs, L.D. Comparison of DIC and LDV for practical vibration and modal measurements. *Mech. Syst. Signal Process.* **2017**, *86*, 2–16. [CrossRef]
24. Beberniss, T.J.; Ehrhardt, D.A. High-speed 3D digital image correlation vibration measurement: Recent advancements and noted limitations. *Mech. Syst. Signal Process.* **2017**, *86*, 35–48. [CrossRef]
25. Yu, L.; Pan, B. Single-camera high-speed stereo-digital image correlation for full-field vibration measurement. *Mech. Syst. Signal Process.* **2017**, *94*, 374–383. [CrossRef]
26. Durand-Texte, T.; Simonetto, E.; Durand, S.; Melon, M.; Moulet, M.H. Vibration measurement using a pseudo-stereo system, target tracking and vision methods. *Mech. Syst. Signal Process.* **2019**, *118*, 30–40. [CrossRef]
27. Barone, S.; Neri, P.; Paoli, A.; Razionale, A.V. 3D vibration measurements by a virtual-stereo-camera system based on a single low frame rate camera. *Procedia Struct. Integr.* **2018**, *12*, 122–129. [CrossRef]
28. Barone, S.; Neri, P.; Paoli, A.; Razionale, A.V.; Bertini, L.; Santus, C. Optical Stereo-System for Full-Field High-Frequency 3D Vibration Measurements Based on Low-Frame-Rate Cameras. In *Lecture Notes in Mechanical Engineering*; Springer: Berlin, Germany, 2019; pp. 155–164._14. [CrossRef]
29. Barone, S.; Neri, P.; Paoli, A.; Razionale, A.V. Low-frame-rate single camera system for 3D full-field high-frequency vibration measurements. *Mech. Syst. Signal Process.* **2019**, *123*, 143–152. [CrossRef]
30. Endo, M.T.; Montagnoli, A.N.; Nicoletti, R. Measurement of Shaft Orbits with Photographic Images and Sub-Sampling Technique. *Exp. Mech.* **2015**, *55*, 471–481. [CrossRef]
31. Barone, S.; Neri, P.; Paoli, A.; Razionale, A.V. 3D acquisition and stereo-camera calibration by active devices: A unique structured light encoding framework. *Opt. Lasers Eng.* **2020**, *127*, 105989. [CrossRef]
32. Neri, P.; Paoli, A.; Razionale, A.V.; Santus, C. Low-speed cameras system for 3D-DIC vibration measurements in the kHz range. *Mech. Syst. Signal Process.* **2022**, *162*, 108040. [CrossRef]
33. Eberl, C. *Digital Image Correlation and Tracking*; MathWorks, Inc., Matlab Central: Natick, MA, USA, 2010.